Columbia International Publishing
American Journal of Modern Chemical Engineering
(2015) Vol. 1 No. 1 pp. 40-54

Research Article

Experimental Investigation and Optimization of Air Sparging on Hollow Fiber Membrane Performance

Qusay F. Alsalhy[1*], Raheek I. Ibrahim[1], Haydar Alaa Salih[1], and Mumtaz A. Zablouk[1]

Received 19 April 2014; Published online 22 November 2014

Abstract

The objective of this study is to promote the performance of the hollow fiber ultrafiltration (UF) membrane using air-liquid two-phase flow to depress the concentration polarization layer. The effect of various operating conditions such as, feed concentration, flow rate, temperature, transmembrane pressure, and air flow rate on UF performance was estimated and optimized. The Win-QSB technique is an interactive system contains powerful tools to solve different type of problems and optimization. The Win-QSB technique with linear and integer programming (LIP) was used for a first time to optimize the operating conditions in order to maximize the objective function as well as developing a mathematical model to predicate the permeate flux. It was found that the permeation flux and the protein rejection throughout the UF process are affected significantly by the operating conditions. The results showed a significant effect of air flow rate on permeate flux and protein rejection. In addition, the results showed that the experimental data have good agreement with the values estimated by the mathematical model for permeate flux. Finally, the optimization result shows that air injected with the feed solution enhances hollow fiber UF membrane permeate flux by a factor of (0.37).

Keywords: Air sparging; Optimization; Separation performance; Ultrafiltration; Hollow fiber membrane

1. Introduction

It is well known that the performance of ultrafiltration is restricted by membrane fouling which causes a significant decline in the efficiency of a separation performance. Therefore, in order to overcome membrane fouling problem, three different methods can be used to improve the membrane separation performance such as air sparging, critical flux, and back-pulsing. Among the aforementioned methods with more effective and low-cost is air sparging method which can be used efficiently to reduce the effect of membrane fouling during ultrafiltration by injected the air

*Corresponding e-mail: qusay_alsalhy@yahoo.com; qusayalsalhy@uotechnology.edu.iq
1* Membrane Technology Research Unit, Department of Chemical Engineering, University of Technology, Alsinaa Street 52, Baghdad, Iraq

into the membrane cell to promote an agitated flow on the active layer of the outer surface of the membrane.

Several researchers focused on the use of air sparging as an effective method to overcome fouling phenomenon in the ultrafiltration membranes (Bellara et al., 1996; Cui et al., 1996; Li et al., 1998; Derradji et al., 2000; Vatai et al., 2007). Their results were emboldening when air was sparged into the membrane cell, with flux enhancements obtained for dextran, Bovine serum albumin (BSA), and human serum albumin (HSA) solution, and oil/water emulsion. Other researchers enhanced the performance of ultrafiltration membrane by injection of nitrogen gas (Um et al., 2001). They found that nitrogen sparging results in promoting turbulence on the membrane surface which in turn improves the permeation flux of the membrane.

Actually, very few researchers focus their studies on the optimization of the operating conditions of membrane separation process (Drews et al., 2010; Alsalhy et al., 2013). The optimum bubble size and air flow rate for fouling control using experimental and numerical methods was determined by (Drews et al. 2010). Whereas (Alsalhy et al., 2013) used the central composite design (CCD) technique to find the optimal operating conditions such as feed concentration, flow rate, temperature, operating pressure, and gas flow rate on the performance of the reverse osmosis (RO) process of simulated seawater in order to reduce the concentration polarization layer.

In the present study several operating conditions, such as transmembrane pressure (TMP), feed concentration, feed solution flow rate, and air bubble flow rate, were used for reducing membrane fouling and improving the BSA solution permeation flux through PVC hollow fiber membranes. For a first time the influences of these conditions on the performance of the ultrafiltration membranes were optimized using Win-QSB/ Version 1.0 package software program to predicate a mathematical model between the operating conditions and permeate flux.

2. Materials and Methods

Figure 1 shows the schematic diagram of the experimental hollow fiber UF membrane unit. This unit is designed to operate air sparging in a hollow fiber UF membrane module. PVC/PS hollow fiber UF membrane was used with specifications is summarized in Table 1. More details about the PVC/PS hollow fiber membrane can be obtained elsewhere (Alsalhy et al., 2013). The UF module was operated vertically with sparging air into the system. Air and feed solution were injected in the module via a vertical pipe (5 mm inner diameter). The feed solution was prepared by dissolving 500, 800, 1100, 1400, and 1700 mg of BSA in 1 L of distilled water using a magnetic stirrer. The feed solution was pumped from a feed tank to the hollow fiber membrane module in a cross-flow filtration and was re-circulated. With the feed solution, air was injected in concurrent flow by using air compressor (AAC-WD2, 220V-50Hz, 1500W, 2850rpm, 50L, 208L/min, serial No. 08093001 made in China). Feed flow rate, airflow rate, and transmembrane pressure were controlled by means of a valve. The feed solution temperature was kept constant at (10 ± 2^{o}C) by using a thermostat. Pure water permeability (PWP) (kg/(m^2 hr bar)) and Bovine Serum Albumin (BSA, MW67,000) rejection (R%) were estimated respectively using the following equations:

$$PWP = \frac{M}{t\ A\ \Delta P} \tag{1}$$

$$R(\%) = \left[1 - \frac{C_P}{C_f}\right] \times 100 \quad (2)$$

where M is the mass of the collected permeate (kg), t is the collected time (h), ΔP is the trasmembrane pressure (bar), A is the effective surface area of the membrane (m^2), C_f and C_p are the solute concentrations in feed and permeate solution, respectively. The concentration of BSA was determined using a Shimadzu UV-1601 double beam spectrophotometer based on absorbance at a wavelength of 280 nm.

The operating conditions were as follows: concentration (500–1700) mg/L, feed flow rates (100–500) L/h, operating pressure (0.4–2) bar and air flow rates (0-400) L/h.

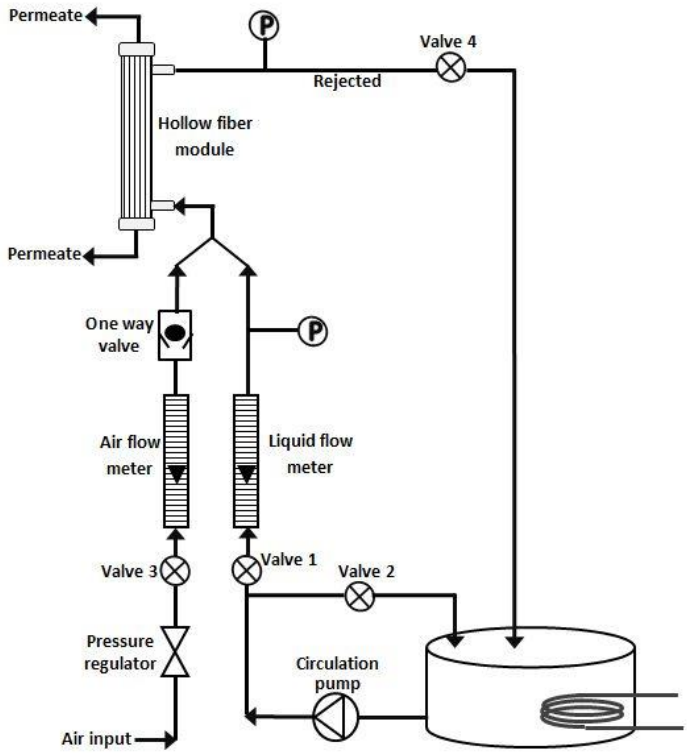

Fig. 1. Schematic diagram of the ultrafiltration experimental unit

Table 1 Specifications of the hollow fiber UF membrane

Material	O.D. (mm)	I.D. (mm)	Thickness (mm)	Porosity (%)	Mean pore size (μm)	Length (mm)	Effective surface area (m^2)
PVC/PS**	1.13	0.61	0.26	82.5	0.381	250	0.0027

**PVC: Poly(vinyl chloride); PS: Polystyrene

3. Optimization and Model Description

The operating variables such as air flow rate (X_1), transmembrane pressure (TMP) (X_2), feed flow rate (X_3) and feed concentration (X_4) were optimized using winQSB technique (winQSB software version 1.0) in order to find the optimum values of operating conditions to promote the permeation flux of the hollow fiber UF membranes. WinQSB is an interactive system contains powerful tools to solve different types of problems in the field of operation research and engineering. The system consists of several modules, one of them is linear and integer programming. There are three methods to solve the Linear Integer Programming (LIP) problems: Graphical method, Algebraic method, and Simplex method. The simplex method is highly sensitive with high efficiency; therefore it was used to solve the linear optimization problem in the present study.
The mathematical formula of linear programming is:

$$Max\ (Min)\ Z = C_1X_1 + C_2X_2 + \cdots\cdots\cdots + C_iX_i + \cdots\cdots\cdots + C_nX_n \quad (3)$$

where Z is the objective function (permeate flux), X_i is the affecting variable, C_i is a numerical coefficient, i=1 ..... n

The linear constrains are defined as:-

$$a_{11}X_1 + a_{12}X_2 + \cdots\cdots\cdots a_{1n}X_n\ (<=,>=,=)\ b_1 \quad (4)$$

$$a_{21}X_1 + a_{22}X_2 + \cdots\cdots\cdots a_{2n}X_n\ (<=,>=,=)\ b_2 \quad (5)$$

$$a_{m1}X_1 + a_{m2}X_2 + \cdots\cdots\cdots a_{mn}X_n\ (<=,>=,=)\ b_m \quad (6)$$

$$X_i >= 0\ \ (i = 1, 2, \ldots\ldots\ldots\ldots n)$$

where, n is number of variables, m is number of constraints.

A 65 linear constrains are made according to each experiment operating conditions and these constrains are represented in a matrix form. The software program was maximizing the objective function (permeate flux) by iteration until the percentage error reach minimum value to fit the suggested linear and integer model equation. Therefore, by using the Linear Integer Programming (LIP), the following model equation for permeates flux was found:

$$Y = 1.4343 + 0.0111X_1 + 0.0181X_2 + 31.1417X_3 + 0.0003X_4 \quad (7)$$

where *Y* represents the permeate flux, X_1 is air flow rate, X_2 is feed flow rate, X_3 is transmembrane pressure, and X_4 is feed concentration. It is worthy to mention here that the mean absolute average error was 0.06294 and correlation coefficient was 0.93713.

4. Two-phase Flow Pattern

In the hollow fiber membrane module Air-Liquid two-phase flow was used to overcome concentration polarization and fouling of the hollow fiber membrane. The concentration polarization is significantly affected by the flow patterns which influences the hydrodynamic conditions near the membrane surface and have an influence on the ultrafiltration performance efficiency. In order to identify the two phase flow pattern in the membranes, the air volume fraction or injection factor (ε) is sometimes used; this factor is calculated according to the following equation:

$$\varepsilon = \frac{U_{GS}}{U_{GS} + U_{LS}} \tag{8}$$

where U_{GS} , U_{LS} are superficial velocities for gas and liquid slugs, respectively.

At values of ε < 0.2 bubble flows is found, while at values of ε > 0.9 annular flows is observed. Besides, Slug flow is appear when 0.2 < ε < 0.9. It is worth to mention here that the Slug flow is the most effective flow pattern for reducing cake layer builds up on the surface of the hollow fiber membranes due to high shear stresses induced by water and air slugs (Alsalhy et al., 2013).

5. Results and Discussion

Figure 2 and Figure 3 show the effects of feed flow rate on the permeate flux and protein rejection of hollow fiber membrane as a function of air flow rate. It can be noticed that increasing feed flow rate from 100 to 500 l/hr without air sparging results in increasing the permeate flux of the hollow fiber membranes from 39 to 45.9 (kg/m^2 s) as shown in Figure 2. Generally, increasing the flow rate of the liquid results in increasing the turbulence of the liquid on the membrane surface, this in turn leads to sweep away the accumulated solute and increasing the permeation flux (Munir, 1998). Moreover, as the air flow rate increased from 100 to 400 l/hr the permeate flux increased. For example, using 100 l/hr the permeate flux increased from 41 to 50.5 (kg/m^2 s), and using 200 l/hr the permeate flux enhanced from 44 to 51.3 (kg/m^2 s), further increase of air flow rates such as 300 and 400 l/hr the permeate flux increased from 47 and 48.5 (kg/m^2 s) to 52 and 52.5 (kg/m^2 s), respectively. Effect of air sparging on enhancing permeation flux and minimizing the effects of concentration polarization of the hollow fiber membrane is attributed to the flux turbulence as a result of the air flowing at the membrane surface in addition to the impact of the shear stresses that are generated between the membrane surface, air and liquid solution (Hemmati et al., 2012; Cabassud et al., 2001). It is worthy to mention here that, the rate of increment of permeation flux declines with increasing of air flow rate inside the hollow fiber membrane module. This phenomenon is attributed to the increase of volume fraction of air in liquid solution (ε) inside the shell of the hollow fiber membrane module as shown in supplementary Figures S1, S2 and S3. In Figure S1A, with injection factor of $(\varepsilon = 0.5)$ the air slugs appear large enough to distinguish a slug flow pattern, while at $(\varepsilon = 0.75)$ air slugs become larger because of high volume fraction of air (see

Figure S1B). In Figure S1C, at injection factor of $(\varepsilon = 0.8)$ the air slugs are highly elongated near the boundary of annular flow regime. For Figure S2, when the injection factors $(\varepsilon = 0.5, 0.6, 0.666)$ in Figure S2A, B, and C, respectively, it can be seen that the flow field is slug flow, whereas increasing of the volume fraction of air resulted to a larger air slugs. In Figure S3A, with injection factor of $(\varepsilon = 0.166)$ a few small size bubbles referred to bubbly flow. Whereas, increasing air volume fraction (injection factor) to 0.375, the air slugs appeared which is formed by the coalescence of small bubbles as shown in Figure S3B. Further increase of the air volume fraction up to $(\varepsilon = 0.444)$ the bubble coarse agglomerated and a slug flow pattern was distinguished (see Figure S3C).

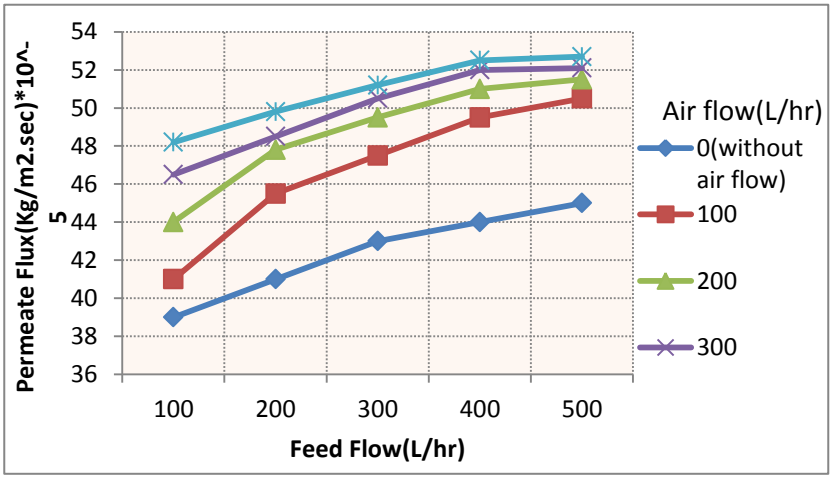

Fig. 2. Effect of feed flow rate on the permeate flux of hollow fiber membranes as a function of air sparging (TMP=1.2bar, feed concentration=500mg/L).

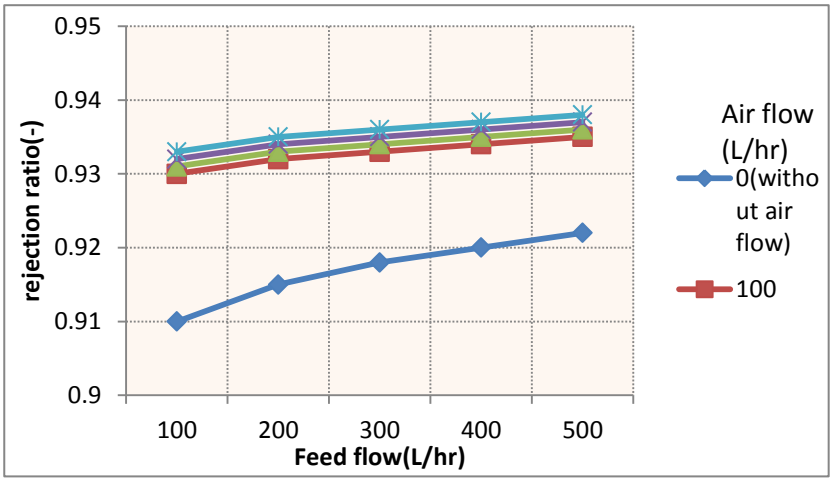

Fig. 3. Effect of feed flow rate on protein rejection of hollow fiber membranes as a function of air sparging (TMP=1.2bar, feed concentration=500mg/L).

Hemmati et al. (2012) reported that increasing the air flow rate results in a decrease of the effective membrane surface area with liquid solution because of the partial acquisition of membrane pores by air bubbles. Moreover, it can be seen from Figure 2 that there is no perceptible effect of the air sparging on the permeation flux using high liquid flow rate such as 400 and 500 l/hr.

From Figure 3, it can be noticed that the protein rejection increases from 0.91 to 0.921 with an increase of feed flow rate from 100 to 500 l/hr without air sparging. When increasing air sparging from 100 to 400 l/hr with feed flow rate from 100 to 500 l/hr the rejection ratio slightly improved and was between 0.93 and 0.942. (Alsalhy et al., 2013and Cui et al., 2003) reported that using air-liquid two-phase flow could potentially increase the recovery of desired products or enhance the quality of the permeate when a high rejection is required.

Figure 4 and Figure 5 show the influence of protein concentration in feed solution on the permeate flux and protein rejection of hollow fiber UF membranes with and without air sparging. It can be noticed that increasing protein concentration from 500 to 1700 mg/L led to a reduction in the permeate flux from 47.5 to 46.1 (kg/m^2 s) without using air sparging as shown in Figure 4. When increasing air sparging with feed side from 100 to 400 l/hr at constant protein concentration in feed solution the permeate flux improved in comparison with that measured without air sparging. The highest value of permeate flux was at protein concentration of 500 mg/L by using 400 l/hr air flow rate. Because of increased turbulence, protein particles accumulated on the membrane surface back transported from the membrane wall to the bulk of the fluid mixture which can result in decreasing the resistance of the concentration polarization on membrane surface and in turn increasing the permeation flux (Huisman et al., 1999). Furthermore, the viscosity of an air-liquid mixture decreased with increasing the air flow rate and accordingly the turbulence in the module shell increased, which in turn resulted in an increase of permeation flux. In Figure 5 it can be noticed that the protein rejection increases with the increase of protein concentration in feed solution from 500 to 1700 mg/L with and without air sparging. The protein rejection increased from 0.918 to 0.952 with increasing of the protein concentration in feed solution without using air sparging. Moreover, there is a similar effect of air flow rate on protein rejection using 200, 300 and 400 l/hr air flow rate in feed side and the rejection ratio was improved from 0.945 to 0.977 as shown in Figure 5.

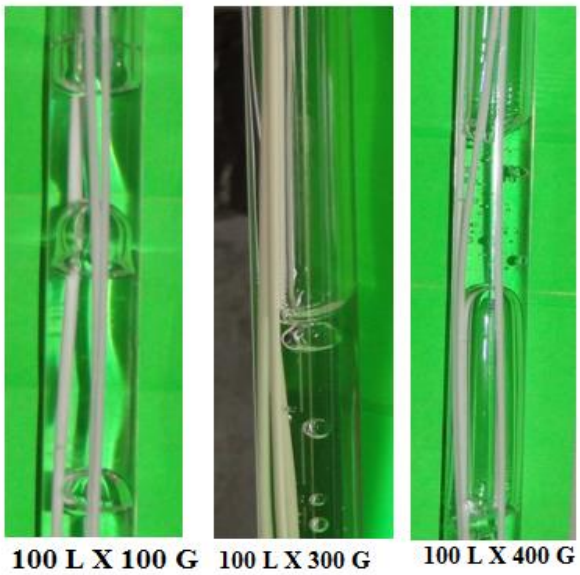

Fig. S1. Pictures of flow pattern in the hollow fiber ultrafiltration module at 100 L/hr feed flow rate and different air flow rates (i.e., 100, 300, and 400 L/hr)

Fig. S2. Pictures of flow pattern in the hollow fiber ultrafiltration module at 200 L/hr feed flow rate and different air flow rates (i.e., 200, 300, and 400 L/hr)

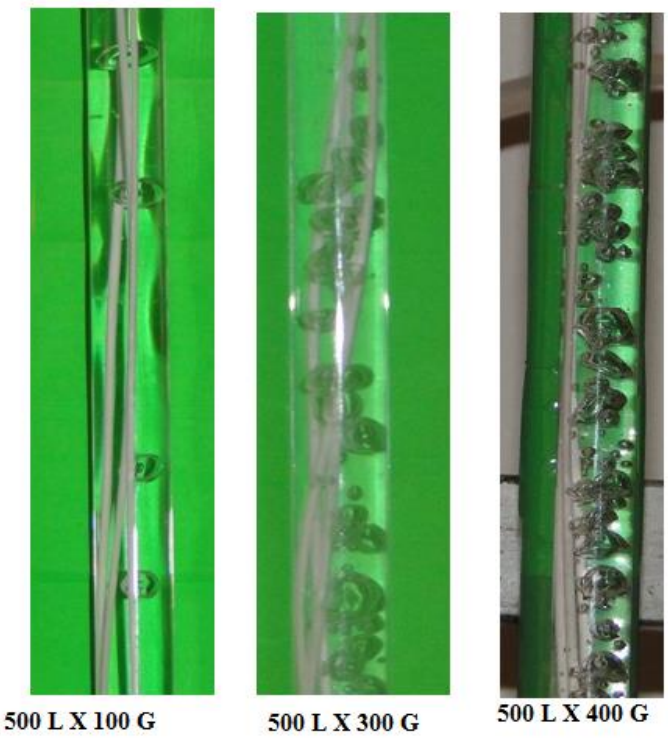

Fig. S3. Pictures of flow pattern in the hollow fiber ultrafiltration module at 500 L/hr feed flow rate and different air flow rates (i.e., 100, 300, and 400 L/hr)

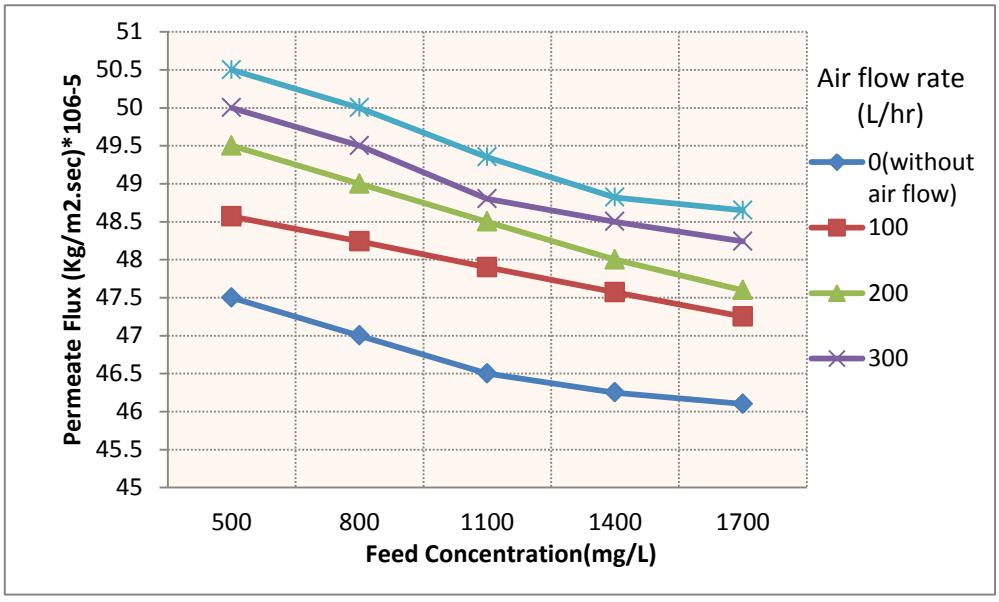

Fig. 4. Effect of feed concentration on permeate flux of hollow fiber membranes as a function of air sparging (TMP=1.2bar, feed flow=300L/hr).

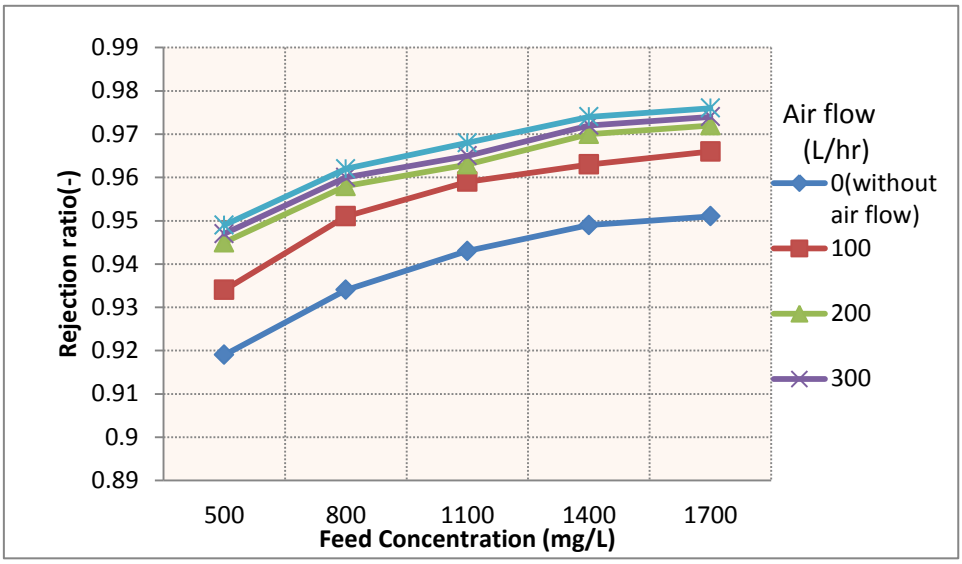

Fig. 5. Effect of feed concentration on protein rejection of hollow fiber membranes as a function of air sparging(TMP=1.2bar, feed flow=300L/hr).

Figure 6 shows the effect of transmembrane pressure on the permeate flux of protein solution as a function of air flow rate. It can be noticed that increasing the transmembrane pressure from 0.4 to 2 bar results in increasing the permeate flux with and without air sparging. (Hemmati et al., 2012) reported that an increase in transmembrane pressure results in increasing the permeation flux because of the higher driving force of the filtration process. The highest value was when using 400 l/hr air flow rate and the permeate flux increased from 28 to 79 (kg/m^2 s). In Figure 7, it can be noticed that the protein rejection decreases with increasing the transmembrane pressure and the protein rejection improved with using air flow rate in feed side. During the membrane separation process the concentration polarization layer (i.e., cake-gel layer) formed on the membranes surface. This cake-gel layer increased with increasing transmembrane pressure, because of the protein molecules deposit on the membrane surface. Moreover, increasing the TMP leads to increase the force on the solute to pass through the membrane which results in decreasing the solute rejection. In fact, Air sparged can strongly minimize the concentration polarization layer (i.e., cake-gel layer) formation on the hollow fiber surface due to the turbulence at the membranes surface as well as the shear stress between the air bubbles and the surface of the hollow fiber membranes as it is mentioned in details above. This phenomenon can moderately describe why the performance of the hollow fiber membranes improved by air sparged.

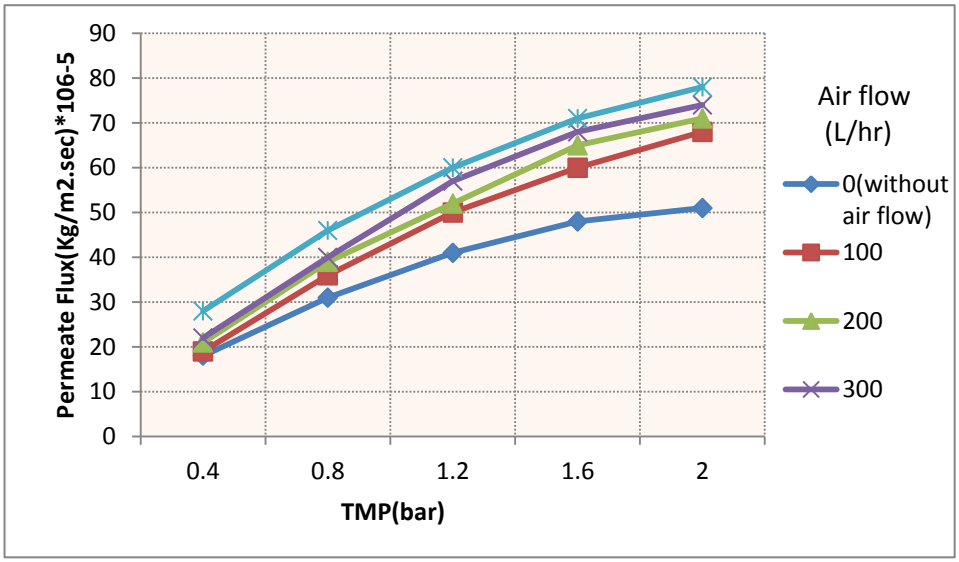

Fig. 6. Effect of transmembrane pressure on permeate flux of hollow fiber membranes as a function of air sparging (feed flow=300L/hr, feed concentration=500L/hr).

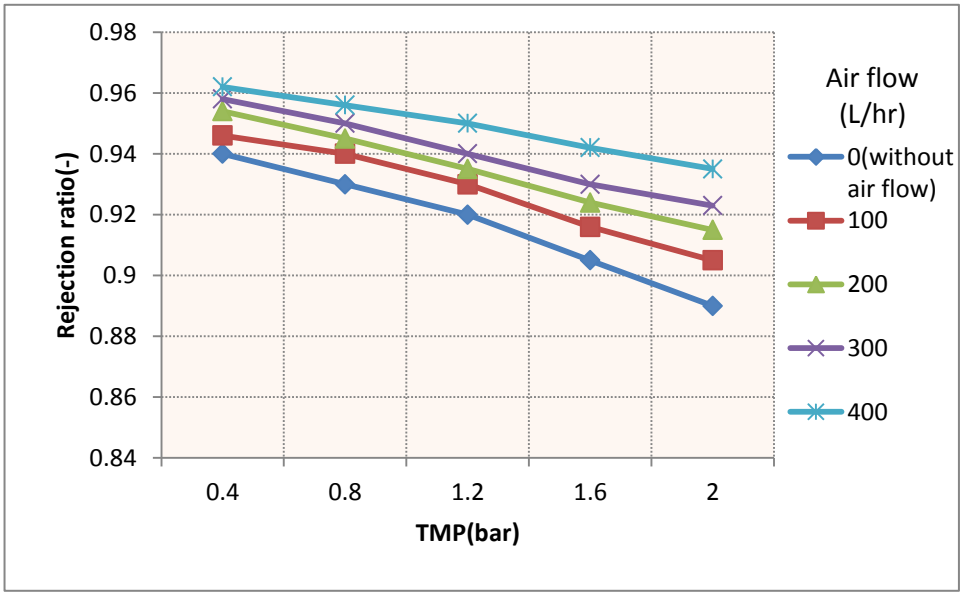

Fig. 7. Effect of transmembrane pressure on protein rejection of hollow fiber membranes as a function of air sparging (feed flow=300L/hr, feed concentration=500L/hr).

Figure 8 shows the optimum conditions of the air flow rates on the permeation flux which may be used with the feed solution to obtain the best performance of the hollow fiber UF membrane. The Optimum conditions for maximum permeation flux were: Air flow rate= 400 (L/hr), Feed flow rate=

300 (L/hr), TMP= 2 (bar), Feed concentration= 500 (mg/L). At these conditions the injection factor was $(\varepsilon = 0.57)$ where slug flow pattern is clearly presented. This value of the air volume fraction (injection factor) led to high shear stresses that are created between the membrane surface, air and liquid solution and in turn enhanced the performance of the hollow fiber membranes.

Figure 9 shows the flux enhancement as a function of air injection at optimum conditions (i.e., feed flow rate= 300 L/hr, TMP= 2 bar, feed concentration= 500 mg/L). It can be seen that the permeation flux increases with increasing the air flow rate in shell side of the hollow fiber membrane module. From Figure 9 it can be concluded that the UF performance of the hollow fibers membrane is enhanced by a factor of 0.37.

Finally, Figure 10 depicts the comparison between the experimental values and theoretical values of the permeation flux of the hollow fiber UF membrane. It can be seen that there is a good agreement between the experimental and theoretical values obtained by the process method presented in this study.

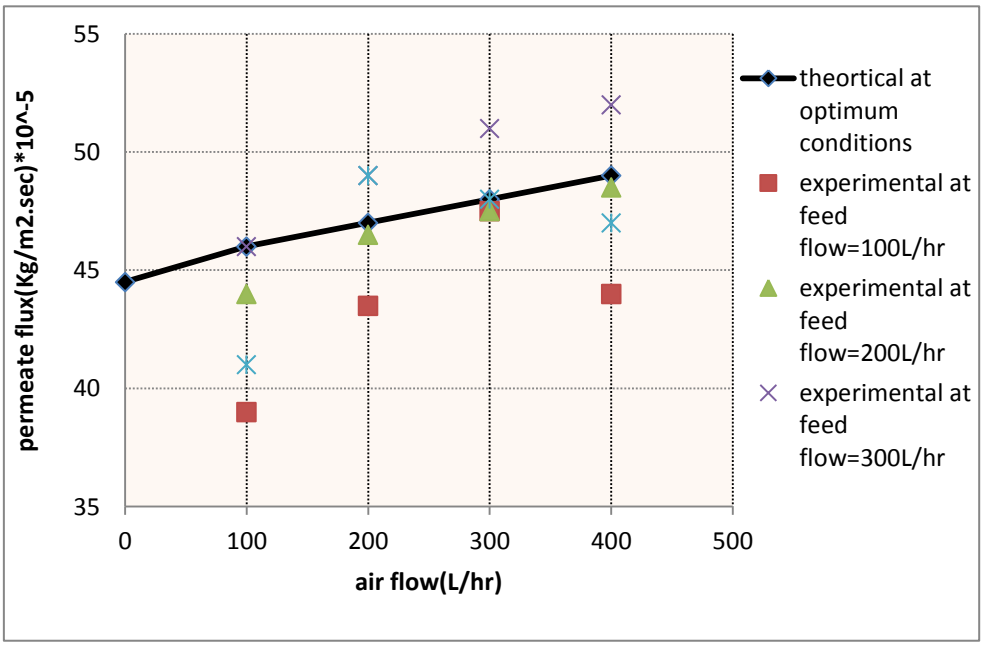

Fig. 8. Effect of optimum air flow rates on the permeation flux of the hollow fiber membranes (TMP=2bar, feed concentration=500mg/L)

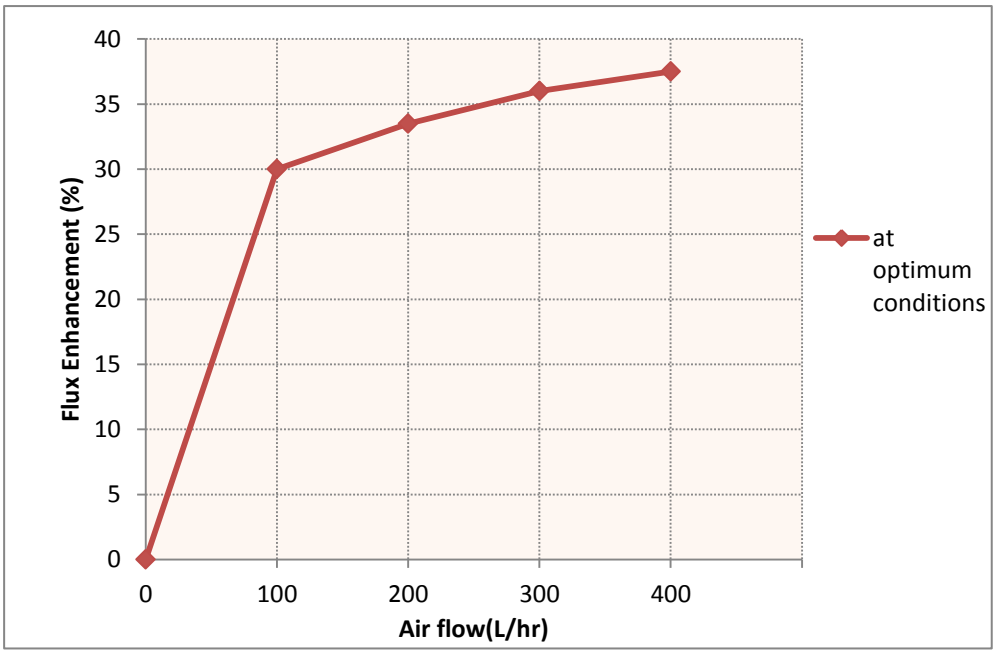

Fig. 9. Flux enhancement percentages as a function of air injection at optimum conditions (feed flow=300 L/hr, TMP= 2 bar, feed concentration =500 mg/L)

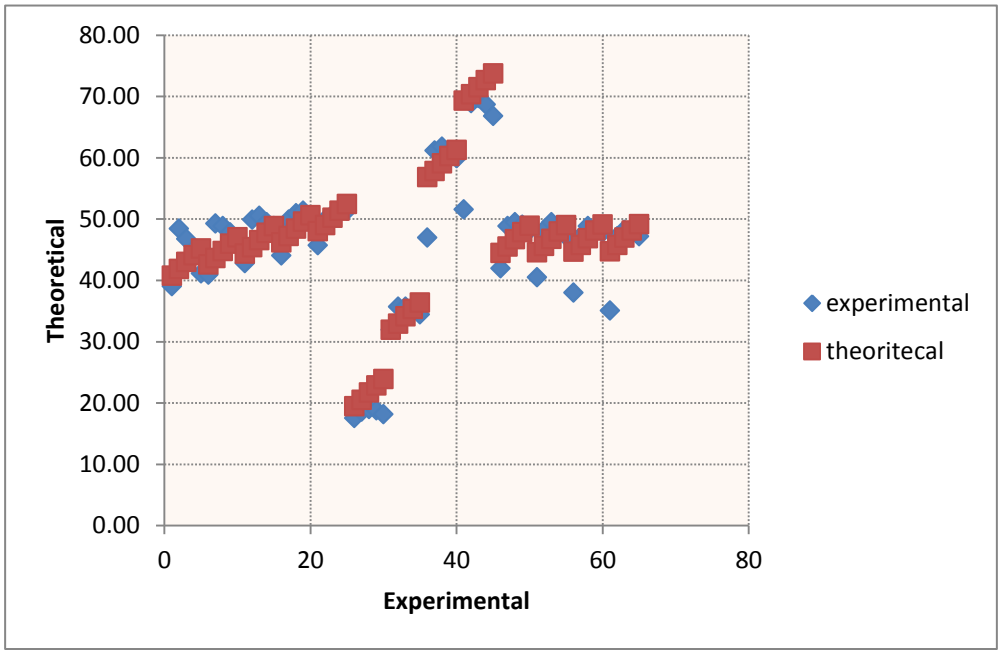

Fig. 10. Comparison between experimental and theoretical values of permeate flux

6. Conclusions

The effects of air flow rate, feed flow rate, feed concentration and transmembrane pressure on the hollow-fiber ultrafiltration membrane performance were studied and optimized. The following conclusions may be towed from the experimental and optimization results:

The experiments depicted that the air injected with the feed solution enhances hollow fiber UF membrane permeation flux by a factor of 0.37, which means that the permeation flux increases by 37%. This effect is attributed to the turbulence and wall shear stress as well as lower fluid mixture viscosity prompts by the air injection.

The influence of air sparging overcome the negative effect of high feed concentration and high transmembrane pressure (TMP) on permeate flux.

A good agreement was found between the experimental and theoretical values within an absolute average error of 0.0629 for the permeation flux of the hollow fiber UF membrane.

References

Bellara, S. R., Cui, Z. F., Pepper, D. S. (1996). Journal of Membrane Science, 121, 175–184. http://dx.doi.org/10.1016/S0376-7388(96)00173-1

Cui, Z. F., Wright, K. I. T. (1996). Journal of Membrane Science, 117, 109–116. http://dx.doi.org/10.1016/0376-7388(96)00040-3

Li, Q. Y., Bellara S. R., Cui, Z. F., & Pepper, D. S., (1998). Sep. Purif. Technol., 14, 79–83. http://dx.doi.org/10.1016/S1383-5866(98)00062-8

Derradji, A.F., Bernabeu-Madico, A., Taha S., & Dorange, G. (2000). Desalination, 128, 223–230. http://dx.doi.org/10.1016/S0011-9164(00)00037-0

Vatai, G. N., Krstic, D. M., Koris, A. K., & Tekic, M. N. (2007). Desalination, 204, 255–264. http://dx.doi.org/10.1016/j.desal.2006.02.034

Um, M.J., Yoon, S.H., Lee, C.H., Chung, K.Y. & Kim, J.J. (2001). Water Res., 35, (17), 4095–4101. http://dx.doi.org/10.1016/S0043-1354(01)00155-5

Drews A., Prieske H., Meyer, E. L., Senger, G., & Kraume, M. (2010). Desalination, 250, 1083–1086. http://dx.doi.org/10.1016/j.desal.2009.09.113

Alsalhy, Q. F., Albyati, T. M., & Zablouk, M. A. (2013). Chemical Engineering Comm., 200, 1–19. http://dx.doi.org/10.1080/00986445.2012.685529

Alsalhy, Q. F., Rashid, K. T., Ibrahim, S. S., Ghanim, A. H., Van der Bruggen, B., Luis, P., Zablouk, M. (2013). Jornal of Applied Polymer Science, 129, 3304- 3313. http://dx.doi.org/10.1002/app.39065

Munir, C. (1998). Ultrafiltration and Microfiltration Handbook, Technomic Publishing Company, Lancaster, Pa.

Hemmati, M., Rekabdar, F., Gheshlaghi, A., Salahi A., & Mohammadi T., (2012). Desalination and Water Treatment, 39, 33–40. http://dx.doi.org/10.1080/19443994.2012.669155

Cabassud C., Laborie, S., L., Durand-Bourlier, & Lainé, J.M. (2001). Journal of Membrane Science, 181, 57–69. http://dx.doi.org/10.1016/S0376-7388(00)00538-X

Cui, Z. F., Chang, S., Fane, A. G. (2003). Journal of Membrane Science, 221, 1–35. http://dx.doi.org/10.1016/S0376-7388(03)00246-1

Huisman, I.H., Tragardh, G., Tragardh, C. (1999). Chemical Engineering Science, 54, 281.
http://dx.doi.org/10.1016/S0009-2509(98)00223-1